

Projections of the Second Cervical Dorsal Root Ganglion to the Cochlear Nucleus in Rats

XIPING ZHAN,¹ TAN PONGSTAPORN,¹ AND DAVID K. RYUGO^{1,2*}

¹Department of Otolaryngology-Head and Neck Surgery, Johns Hopkins University School of Medicine, Baltimore, Maryland 21205

²Department of Neuroscience, Johns Hopkins University School of Medicine, Baltimore, Maryland 21205

ABSTRACT

Physiological, anatomical, and clinical data have demonstrated interactions between somatosensory and auditory brainstem structures. Spinal nerve projections influence auditory responses, although the nature of the pathway(s) is not known. To address this issue, we injected biotinylated dextran amine into the cochlear nucleus or dorsal root ganglion (DRG) at the second cervical segment (C2). Cochlear nucleus injections retrogradely labeled small ganglion cells in C2 DRG. C2 DRG injections produced anterograde labeling in the external cuneate nucleus, cuneate nucleus, nucleus X, central cervical nucleus, dorsal horn of upper cervical spinal segments, and cochlear nucleus. The terminal field in the cochlear nucleus was concentrated in the subpeduncular corner and lamina of the granule cell domain, where endings of various size and shapes appeared. Examination under an electron microscope revealed that the C2 DRG terminals contained numerous round synaptic vesicles and formed asymmetric synapses, implying depolarizing influences on the target cell. Labeled endings synapsed with the stalk of the primary dendrite of unipolar brush cells, distal dendrites of presumptive granule cells, and endings containing pleomorphic synaptic vesicles. These primary somatosensory projections contribute to circuits that are hypothesized to mediate integrative functions of hearing. *J. Comp. Neurol.* 496:335–348, 2006. © 2006 Wiley-Liss, Inc.

Indexing terms: auditory; axoaxonic and axodendritic synapses; granule cells; somatosensory; unipolar brush cells

The cochlear nucleus is the sole recipient of auditory nerve fibers from the cochlea and initiates all ascending auditory pathways in the brain. As the gateway to the central auditory system, it is also noteworthy that this nucleus serves as a multimodal recipient of nonauditory inputs from such structures as the pontine nuclei (Ohlrogge et al., 2001), cuneate nucleus (Itoh et al., 1987; Weinberg and Rustioni, 1987; Wright and Ryugo, 1996; Li and Mizuno, 1997b), spinal trigeminal nucleus (Li and Mizuno, 1997a; Wolff and Künzle, 1997; Haenggeli et al., 2005), vestibular nerves (Newlands and Perachio, 2003) and cervical spinal nerves (Pfaller and Arvidsson, 1988), and dorsal raphe nucleus (Ye and Kim, 2001). These inputs converge on and are processed in the granule cell domain (GCD), whose constituent neurons in turn project to the principal efferent cells of the dorsal cochlear nucleus (DCN; Mugnaini et al., 1980b). To understand how these nonauditory systems influence auditory processing, a first step is to learn about the synaptic organization of the inputs to the GCD.

Electrical stimulation of cervical spinal nerves produced evoked responses in cat DCN neurons, with the largest effect arising from the second cervical level (C2; Kanold and Young, 2001). The spinal nerve at C2 contains proprioceptive and cutaneous fibers that originate from muscle and skin receptors associated with the pinna and neck. It also gives rise to substantial projections to the spinal cord, dorsal column nuclei, and spinal trigeminal nuclei (Pfaller and Arvidsson, 1988; Neuhuber and Zenker, 1989; Pri-

Grant sponsor: National Institutes of Health; Grant number: RO1 DC04395

*Correspondence to: David K. Ryugo, Center for Hearing and Balance, Johns Hopkins University, 720 Rutland Avenue, Baltimore, MD 21205. E-mail: dryugo@jhu.edu

Received 12 September 2005; Revised 21 October 2005; Accepted 30 November 2005

DOI 10.1002/cne.20917

Published online in Wiley InterScience (www.interscience.wiley.com).

hoda et al., 1991). The latter two structures have demonstrated a robust projection to the GCD (Wright and Ryugo, 1996; Haenggeli et al., 2005). It has been suggested that the afferent system entering the upper cervical cord plays a role in tonic and righting reflexes (Abrahams et al., 1984), an idea that is consistent with the hypothesis that cervical and cranial somatosensory afferents are integrated in the DCN to accommodate head and pinna movements on sound-localization cues (Kanold and Young, 2001; Oertel and Young, 2004).

The GCD has emerged as a structure involved in the integration of multimodal afferents with auditory processing. It is not homogeneous with respect to its composition of cell types and endings. Which kinds of afferent endings—boutons or mossy fibers—synapse with which classes of GCD neurons? Learning about the GCD and its neuronal circuits will contribute to our understanding of how visual, vestibular, proprioceptive, motor, and aminergic systems contribute to circuits underlying our perception of sound. One function of polysensory integration would be to help localize sound sources under demanding conditions (e.g., movement of the sound source and/or the listener). Another would be to facilitate selective listening using sound localization cues in noisy backgrounds or to enhance incoming signals by filtering self-generated sounds. In this context, we examined the nature of the dorsal root ganglion (DRG) projections to the cochlear nucleus and asked the following questions. 1) Where in the cochlear nucleus do the C2 axons project? 2) What is the synaptic nature of the endings? (3) What is the neuronal target(s) of the projections?

MATERIALS AND METHODS

This report is based on data from eight adult male Sprague-Dawley rats with histological confirmation of the injection and/or recording sites. Rats (250–380 g) were anesthetized by intraperitoneal injection of sodium pentobarbital (45 mg/kg body weight). Once animals were reflexic to tail or paw pinches, anesthetized animals were positioned in a stereotaxic device and surgery commenced. Supplemental doses of sodium pentobarbital were administered as needed. Five rats had injections of biotin dextran amine (BDA) and/or FluoroGold into the C2 DRG; two rats received a cocktail injection of BDA and FluoroGold into the cochlear nucleus; one rat received an injection of BDA in the cochlear nucleus. All procedures adhered to NIH guidelines and were approved by the John Hopkins University Animal Care and Use Committee.

Electrophysiological recording

The DCN was targeted by stereotaxic coordinates (Paxinos and Watson, 1998) or by exposing the DCN by aspiration of part of the cerebellum. Calibrated stimuli (tones, clicks, or noise) were delivered via free-field speakers using Tucker-Davis System III hardware. Single- and multiunit recordings were made from micropipettes filled with 0.01 M Tris buffer, 2 M NaCl, and 10% BDA (pH 7.6). Thresholds and best frequencies (that frequency to which the unit was most sensitive) were collected by using an automated tuning curve maker. Impedances were 2–5 M Ω . At the end of the recording session, injections were made by passing 5 mA of positive current for 10 minutes (50% duty cycle). The pipette was left in place for 10

minutes after the current was turned off and then was withdrawn.

Injection procedure

The cervical vertebrae were exposed after a midline incision and dissection of the neck muscles. The first vertebra was partially removed to expose the C2 DRG or spinal nerve. The ganglion or spinal nerve was injected by using a glass micropipette (tip diameter 40–60 μ m) filled with a mixture of 15–20% BDA and 2% FluoroGold solution (Molecular Probes, Eugene, OR) in 0.01 M TBS or 15–20% BDA alone. A small deposit of the tracer (50 nl) was delivered via an oocyte injector (NanoInjector; Drummond Instruments). Multiple injections of tracer were made in the DRG with a total injection volume of 0.6–1.2 μ l. After each injection, the pipette was left in situ for 5–6 minutes before being withdrawn. When all injections were complete, the exposed muscle and skin were cleaned, the skin was sutured, and the animal was allowed to recover.

Histological processing

After a survival of 3–15 days, the rats were deeply anesthetized with an overdose of pentobarbital (90 mg/kg body weight) and transcardially perfused with 300–450 ml of chilled fixative (4% paraformaldehyde in 0.12 M PB, pH 7.3). Dissected brains were postfixed in the same fixative for 1–2 hours, embedded in gelatin-albumin, and cut in the transverse plane. Serial sections (60 μ m thickness) of the lower brainstem, cerebellum, and spinal cord were collected in culture wells containing 0.12 M PB (pH 7.3). The C2 DRG was removed, flattened, and transferred to a separate well in PB or embedded with the brain tissue for cutting. Sections were treated with biotinylated peroxidase-avidin complex (ABC-Elite; Vector, Burlingame, CA) containing 0.05–0.1% Photo-Flo (Kodak) to permeabilize the tissue. A nickel-diaminobenzidine (DAB) method (0.0125% DAB, 0.25% nickel ammonium sulfate, and 0.35% imidazole in 0.05 M cacodylate, pH 7.2) was used for visualizing the reaction. Reacted sections were examined by light microscopy. Those sections that contained examples of labeled fibers and endings were set aside for processing for electron microscopy. The remaining sections were mounted on gelatin-coated microscope slides, counterstained with cresyl violet, and coverslipped with Permount.

EM studies

The selected sections were osmicated in 1% OsO₄ in 0.1 M PB (pH 7.4) for 15 minutes, rinsed in 0.1 M maleate buffer (pH 5.2), stained in 1% uranyl acetate for 15 hours, rinsed in buffer, dehydrated in alcohols, and flat embedded in Epon between sheets of Aclar. Light microscopic maps of these smaller sections were made for orientation purposes, using blood vessels and labeled structures as landmarks to locate the labeled endings. We dissected specific regions containing labeled endings from the tissue sections and reembedded these smaller pieces in BEEM capsules for ultrathin sectioning and analysis with an electron microscope. Serial ultrathin sections were collected on Formvar-coated slotted grids. Sections were studied and photographed using a Hitachi H-7600 electron microscope.

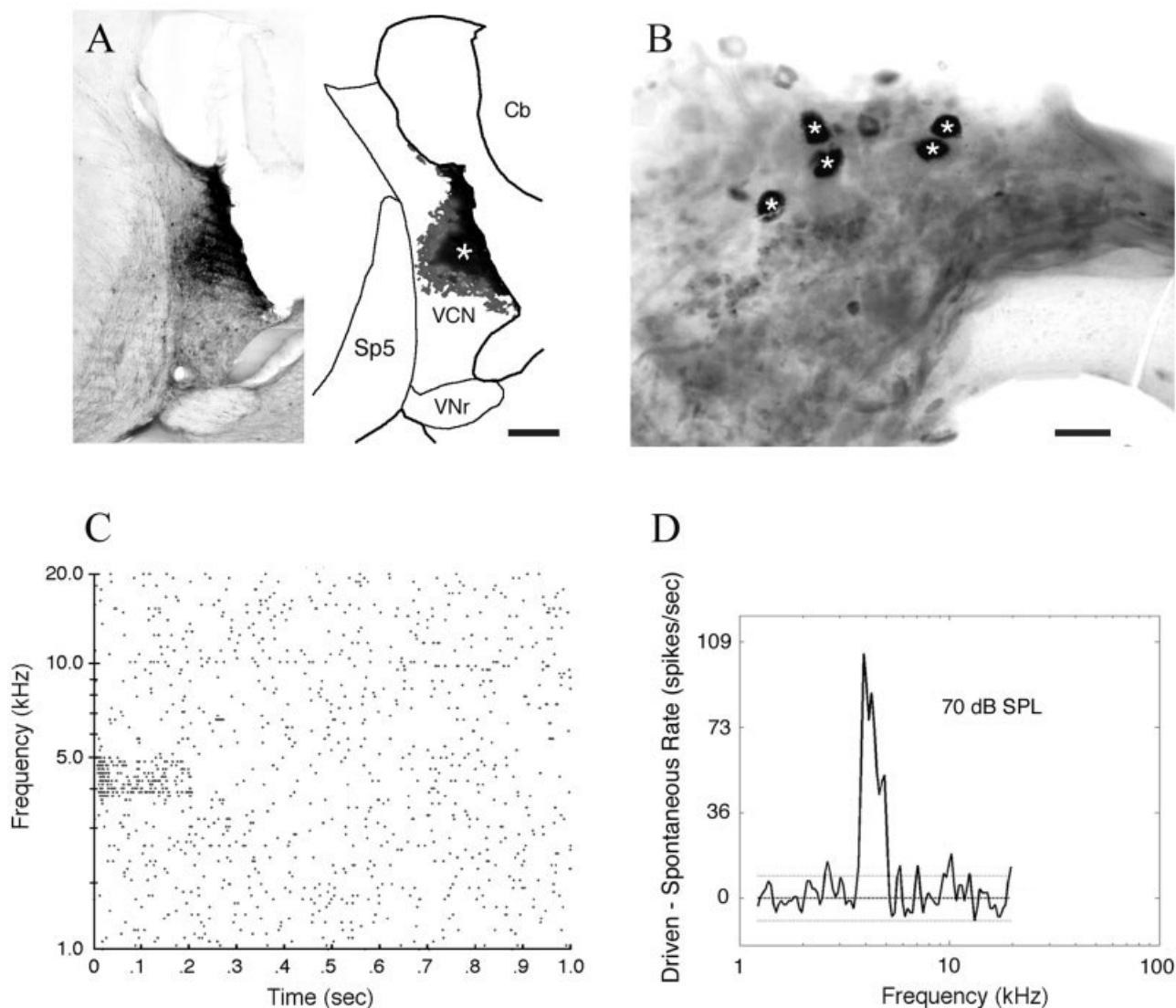


Fig. 1. Retrograde labeling in C2 DRG. **A:** Photomontage (left) and drawing (right) of injection site. The center of the injection site of BDA is located in the AVCN and extends in both directions yet is confined to the CN. It encroaches on the SPC posteriorly. **B:** Photomicrograph showing retrogradely labeled ganglion cells (asterisks) in C2 DRG. The relatively small somatic size suggests that these ganglion cells belong to the type B category. **C:** Raster plot of spikes in response to

200-msec tones of various frequencies at 70 dB SPL. The evoked spike rate is well above the spontaneous rate when the tone is within the unit's response area. **D:** On the basis of the maximal evoked spike discharge and minimal first spike latency, this unit was assigned a best frequency of 3.9 kHz. Dotted lines indicate 2 SD above and below the spontaneous discharge rate. Scale bars = 200 μ m in A; 25 μ m in B.

Data analysis

Montages of tissue sections were made in NeuroLucida software (MicroBrightField Ltd., Essex, VT) with a light microscope, and anterogradely labeled fibers and swellings were plotted. Electron micrographs were examined from previously drawn maps of the cochlear nucleus. Cell type identifications were made on the basis of criteria previously published (Mugnaini et al., 1980a; Floris et al., 1994; Weedman et al., 1996; Diño et al., 2000).

All micrographs were collected with digital cameras. Electron micrographs were collected by using an AMT XR-100 (2,600 \times 2,600, 23- μ m pixel size) and saved as TIFF documents. Light micrographs were collected by us-

ing a chilled, 3-CCD color Hamamatsu 5810 camera and saved as Photoshop documents. All images were optimized in Photoshop, in which contrast and/or brightness were adjusted as needed.

RESULTS

Retrograde labeling in the C2 DRG

Dye injections were guided by electrophysiological criteria, stereotaxic coordinates, or direct visualization. All injection sites for this report were confirmed histologically in which injections of BDA and/or FluoroGold were completely restricted to the cochlear nucleus (Fig. 1A) and

there was retrograde labeling of ganglion cells in the ipsilateral C2 DRG (Fig. 1B). The labeled cell bodies were small, ranging from 15 to 20 μm in diameter, and infrequent in number (18–40 per case). The reaction product obscured the staining features of the cytoplasm, but stained cells fit the size of the so-called type B cells (Rambourg et al., 1983; Tandrup 2004). Electrophysiological recordings immediately prior to the tracer injections confirmed that the auditory structures under study were in good condition (Fig. 1C,D). Single units exhibited spontaneous discharges and evoked responses to suprathreshold pure tones over a range of 3.9–5 kHz. At the end of the recording session, BDA was injected into the cochlear nucleus. Each injection included some part of the GCD and the overlying DCN.

Projection from C2 DRG to the brainstem nuclei

We have five animals with injections confined to the C2 DRG (Fig. 2A). Each injection resulted in darkly labeled fibers and endings in the cuneate nucleus (Cun, Fig. 2B), external cuneate nucleus (ECu; Fig. 2C), nucleus X (Fig. 2C), central cervical nucleus, and lateral areas of the dorsal horn. No labeled fibers were observed in the deep cerebellar nuclei or cerebellar cortex. These results were consistent with a previous report (Pfaller and Arvidsson, 1988) and provided positive controls for the modest but reliable projection observed to the ipsilateral cochlear nucleus in each animal.

The projection to the cochlear nucleus was concentrated within the subpeduncular corner (SPC) of the GCD (Figs. 2D, 3) and lamina (Fig. 2E) with a sprinkling of terminals in the medial sheet and superficial lamina. The SPC resides along the dorsal ridge of the AVCN, immediately beneath the ICP. The lamina represents the caudal and lateral extension of the SPC that separates the VCN from the DCN. The medial sheet is a thin extension of the SPC and lamina that dips down along the medial border of the ventral cochlear nucleus. Labeled swellings in the posterior SPC and medial sheet had a location that was previously identified as the “ventral cochlear nucleus” (Pfaller and Arvidsson, 1988). These terminals in the cochlear nucleus were concentrated in these compartments of the GCD, with just a few labeled boutons found in deep DCN. The endings appeared in various sizes and shapes (Fig. 3).

Pathway of C2 DRG projection to the cochlear nucleus GCD

We followed labeled axons from C2 DRG through the C2 spinal nerve root, into the C2 spinal cord segment to the cochlear nucleus through serial sections. Fibers entered the dorsal horn of spinal cord, where they gave rise to collaterals in layers I–III of lateral dorsal horn. The main DRG fibers ascended in the dorsal portion of the spinal trigeminal tract and passed through nucleus X to enter the cuneate and external cuneate nuclei. These fibers gave rise to collateral projections with swellings that were distributed in close apposition to the somata. Fibers arborized in nucleus X as they projected along the spinal trigeminal tract. The distribution of labeled axons and terminals was plotted for all animals, and a representative case is shown for the cochlear nucleus (Fig. 4). Some fibers traveled laterally to terminate in the posterior SPC (Fig. 4B–D), whereas others curved more rostrally to terminate in the anterior SPC (Fig. 4G–I). Fibers from both

bundles terminated in the GC lamina (Fig. 4H,I). Under the light microscope, labeled endings in the SPC resembled those found elsewhere in the CN and brainstem in terms of size and shape.

EM analysis of labeled endings

The labeled terminals in the GCD were marked by electron-dense precipitate from the DAB reaction product and so are distinct from unlabeled structures (Fig. 5). The structure of the labeled endings was irregular, and they formed multiple contacts with various structures. The structure was indeed more complicated than what the smooth contours suggested from light microscopic images. We selected 23 endings from the SPC, lamina, and medial sheet from three rats for analysis (Table 1). Some endings were selected because of their large size, whereas others were selected at random. These endings exhibited a range of sizes and shapes and did not fall easily into separate categories (e.g., bouton vs. mossy fiber). An ending could appear small or large depending on the orientation and/or location of the cut.

Labeled endings were characterized by a central core of mitochondria, asymmetric membrane specializations, and an abundant supply of round synaptic vesicles. Nearly 75% of the endings made synaptic contacts with more than one target (Table 1). Synaptic relationships were formed with dendrites of unknown origin (Fig. 6A), although they had the characteristics of granule cell dendrites because of their relationship to the ending, their smaller caliber, and their tendency to emit “hair-like” protrusions that invaded the ending (Fig. 6B). Other synapses were found on dendrites that contained ribosomes (Fig. 7). Ribosomes (polyribosomes) are typically found in the cell body but can be associated with the dendritic spine apparatus (Steward and Worley, 2001) and dendrites of the unipolar brush cell (UBC) in the cerebellum and cochlear nucleus (Jaarsma et al., 1996; Diño and Mugnaini, 2000). We observed an unambiguous case in which a labeled ending synapsed onto a UBC dendrite (Fig. 8). The cell body was approximately 8 μm in diameter, exhibited a deep invagination of its nuclear envelope, and emitted a single dendrite that was rich in polyribosomes. This postsynaptic target was reconstructed through serial-section electron micrographs, and the primary dendrite of the unipolar brush cell had multiple dendrites erupting from a location near the labeled ending. This dendritic arrangement is characteristic of UBC morphology (Floris et al., 1994; Wright et al., 1996; Jaarsma et al., 1998). Therefore, we assigned the dendrites containing ribosomes to the class of UBCs.

The other synaptic targets of labeled DRG endings were structures that contained pleomorphic synaptic vesicles (Fig. 9). The power of serial-section analysis is that individual structures can be followed until some unique characteristic is revealed. In this case, postsynaptic structures containing pleomorphic vesicles were identified as synaptic endings by virtue of their continuity with unmyelinated axons and their formation of symmetric membrane specializations with dendritic structures. Because of the intracellular label in the primary afferents, it was not always possible to discern their membrane thickenings. The terminals containing pleomorphic synaptic vesicles, however, exhibited membrane thickenings that were not intimately associated with synaptic vesicles. As a result, we refer to these membrane thickenings as *postsynaptic* to the labeled DRG ending. Eight of twenty-three DRG end-

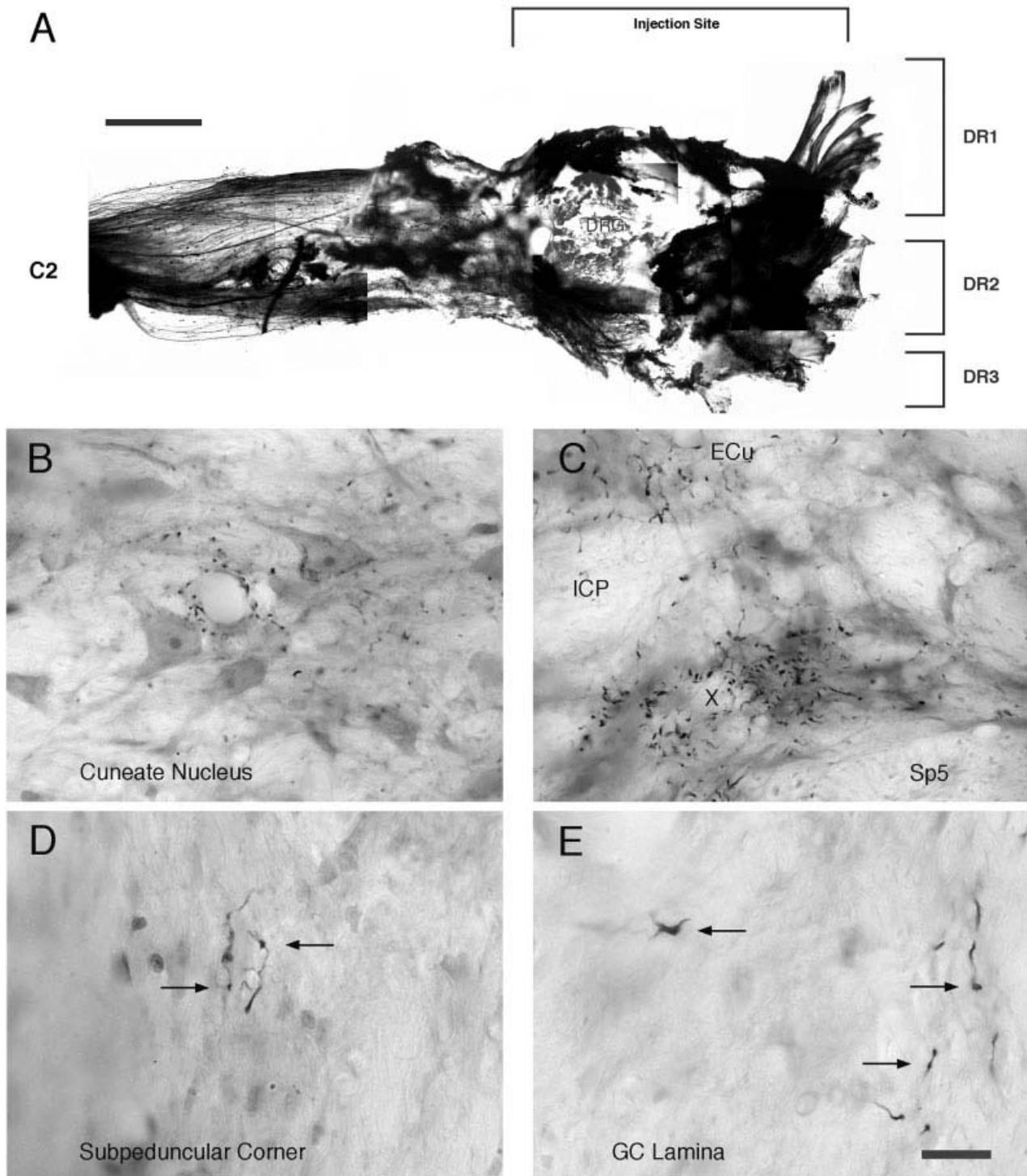


Fig. 2. Anterograde labeling from the C2 DRG to the brainstem. **A:** Photomontage of the injection site in the C2 DRG. The whole-mount preparation also illustrates three rootlets that project into the brainstem (DR1, DR2, DR3). Note the labeled axons that are clearly shown in the peripheral nerve (C2). **B:** Photomicrograph of BDA-labeled fibers and terminals in the ipsilateral cuneate nucleus. **C:** Photomicrograph of labeled fibers and terminals in nucleus X (X

and the external cuneate nucleus (ECu). The terminal field is squeezed between the inferior cerebellar peduncle (ICP) and the dorsal aspect of the spinal trigeminal tract (Sp5). **D:** Photomicrograph of labeled fibers and swellings (arrows) in the subpeduncular corner of the cochlear nucleus GCD. **E:** Photomicrograph of labeled fibers and swellings (arrows) in the lamina of the GCD. Scale bars = 0.5 mm in A; 10 μ m in B (applies to B-E).

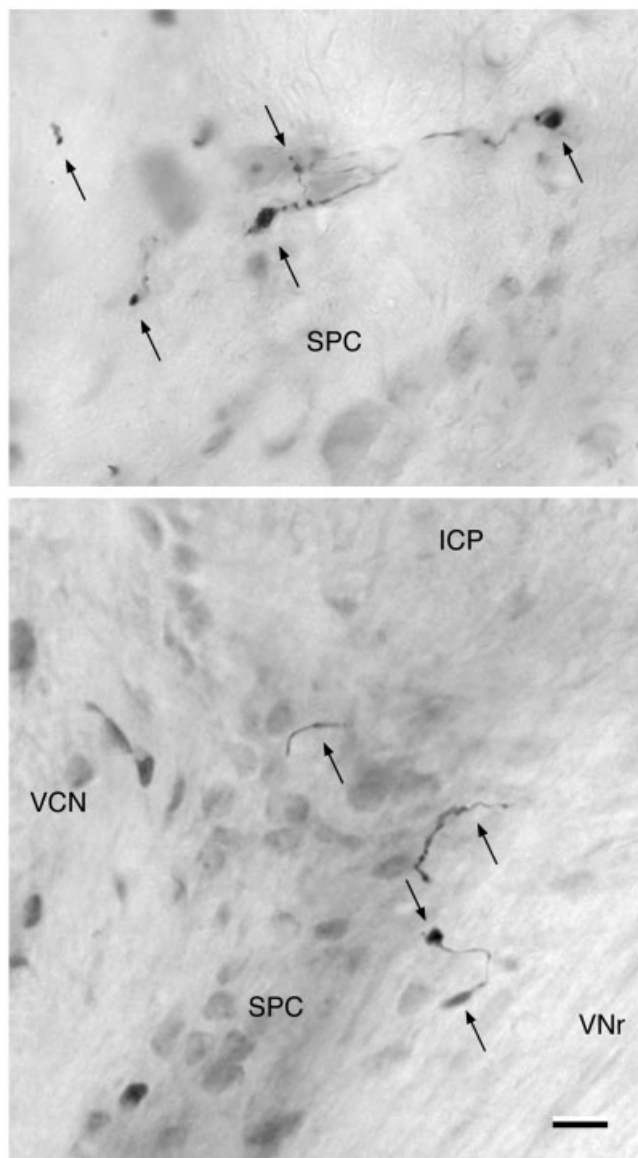


Fig. 3. Photomicrographs of labeled fibers and swellings (arrows) in the subpeduncular corner (SPC) of the GCD. The SPC lies beneath the inferior cerebellar peduncle (ICP) and between the dorsal-medial extent of the ventral cochlear nucleus (VCN) laterally and the vestibular nerve root (VNr) medially. Most of the swellings are small (2–3 μm), but some appear as larger rosettes (4–8 μm). Scale bar = 10 μm (applies to all).

ings gave rise to a total of 19 axoaxonal synapses. DRG terminals that synapsed on axons also tended to form synapses with UBC and presumptive granule cell dendrites (Table 1).

DISCUSSION

Our observations of anterograde and retrograde labeling demonstrate a direct axonal connection between the DRG at the level of the second cervical spinal segment (C2) and the ipsilateral cochlear nucleus. Injections of

BDA or FluoroGold in the cochlear nucleus resulted in the retrograde labeling of spinal ganglion cells at C2. The labeled cells belonged to the general category of type B cells on the basis of their small diameters (Rambourg et al., 1983; Tandrup, 2004). Type B cells are inferred to have unmyelinated or lightly myelinated fibers, but a conclusive relationship among fiber diameter, cell body size, and sensory modality has not been established (Tandrup, 1995; Rustioni, 2005). Moreover, injections of BDA in the DRG produced anterograde labeling of axons and terminals in the ipsilateral cochlear nucleus, specifically within the GCD. There was no label in the magnocellular core of the cochlear nucleus.

Technical considerations

BDA is preferred over neurobiotin and *Phaseolus vulgaris*-leucoagglutinin as axonal tracers for the study of central projections of DRG (Novikov, 2001). The distribution of BDA-labeled swellings from all cases was identical for the spinal cord and brainstem nuclei such as the cuneate nucleus, external cuneate nucleus, and nucleus X, but only pressure injections produced labeled swellings in the cochlear nucleus. Retrogradely labeled motoneurons were consistently found in the ventral horn of the spinal cord, which is also in agreement with previous findings (Pfaller and Arvidsson, 1988; Novikov, 2001). Moreover, survival times longer than 24 hours were required to label DRG terminals in the cochlear nucleus, although labeling in the spinal cord and medulla nucleus was similar regardless of survival time.

The modest nature of this projection merits further discussion. Injections of BDA in the cochlear nucleus produced between 18 and 40 total labeled neurons in the DRG. This relatively low number might be explained by our injection sites not being centered on the terminal field. Our results revealed that most terminals were located in the SPC corner of the GCD. We did not place our injections directly in the SPC, in part to avoid possible contamination by fibers of the inferior cerebellar peduncle or the spinal trigeminal tract. A corresponding concern is why the anterograde projections to the cochlear nucleus were relatively modest. The cell bodies of sensory ganglia neurons are completely invested by simple sheaths composed of single and sometimes multiple layers of satellite cells (Pannese, 1981; Peters et al., 1991). The sheath presumably obstructs intracellular access of the BDA and so limits the ability of the tracer to stain the projections. The small size of the sensory ganglion itself makes leaking of the tracer inevitable after the injection. Thus the volume and concentration of tracer are reduced. These factors may all contribute to a lower uptake efficiency and modest degree of axon labeling.

Projection terminal fields

Our results demonstrated the relatively discrete nature of a projection from the second DRG to the cochlear nucleus. The main projection of the upper cervical DRG is to the external cuneate nucleus. Additional prominent projections are found within the substantia gelatinosa and central cervical nucleus of the spinal cord, medial and inferior vestibular nuclei, nucleus X, nucleus of the solitary tract, perihypoglossal nuclei, and spinal trigeminal nucleus (Pfaller and Arvidsson, 1988; Neuhuber and Zenker, 1989; Prihoda et al., 1991). Our data are consistent with these known projections that serve as positive con-

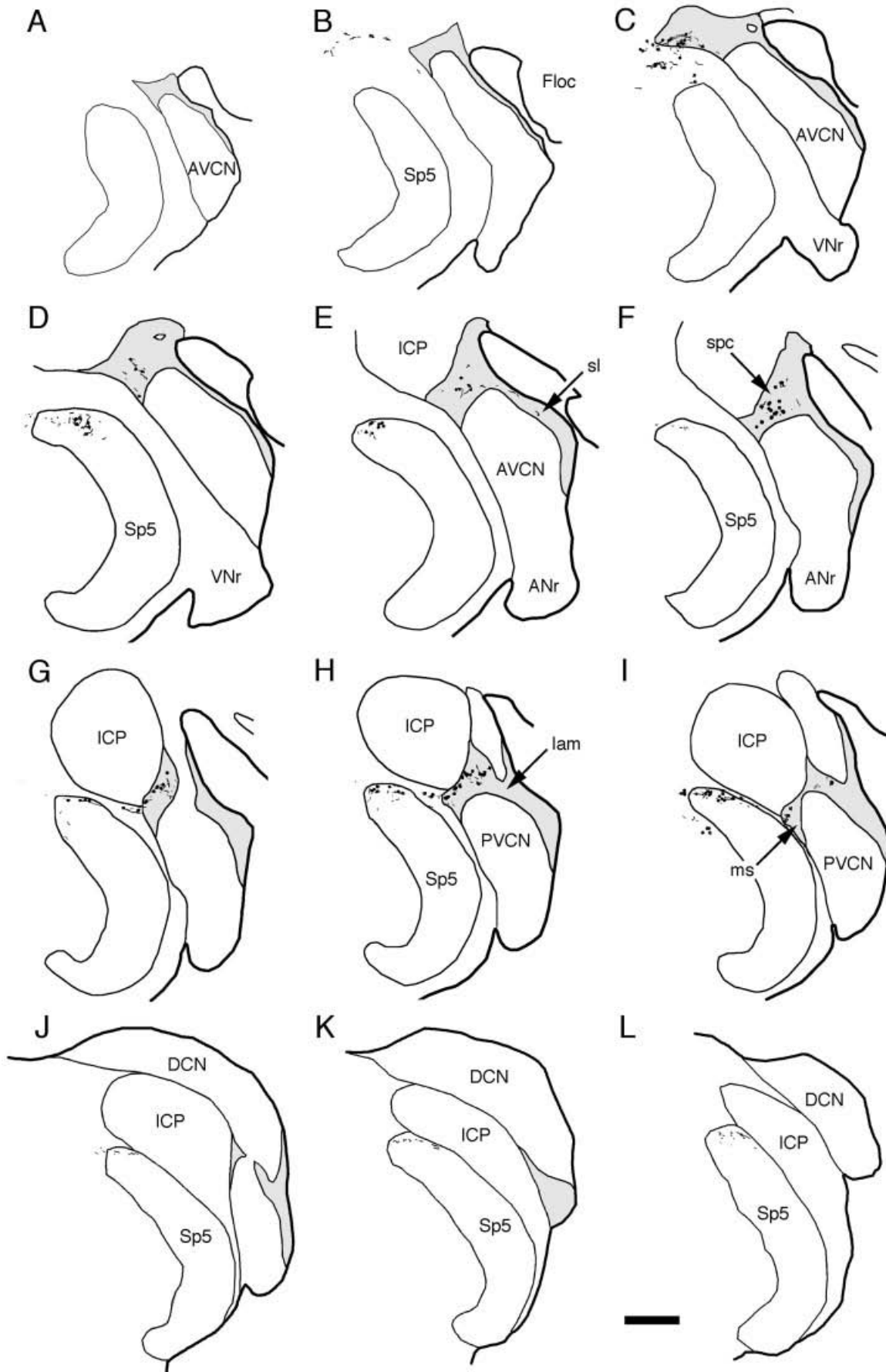


Fig. 4. **A-L:** Drawings of sections through the cochlear nucleus illustrating distribution of labeled axons and terminals in the GCD (shaded gray). Sections are spaced 120 μ m apart. Typically, projections from C2 DRG were concentrated in the subpeduncular corner (spc), medial sheet (ms), superficial lamina (sl), and lamina (lam).

ANr, auditory nerve root; AVCN, anteroventral cochlear nucleus; DCN, dorsal cochlear nucleus; Floc, flocculus of the cerebellum; ICP, inferior cerebellar peduncle; Sp5, spinal tract of the trigeminal nerve, VNr, vestibular nerve root. Scale bar = 0.5 mm in L 9applies to A-L.

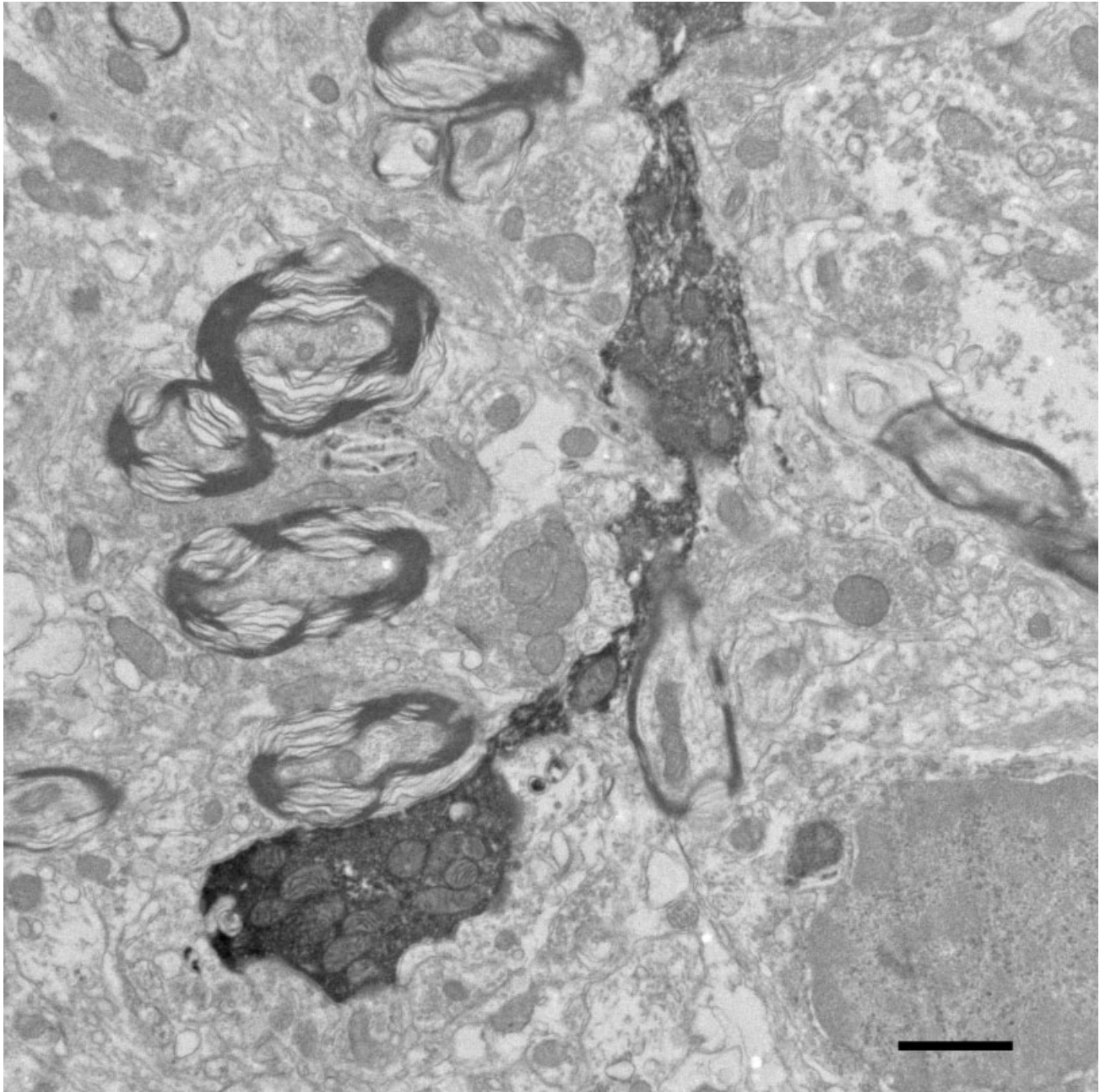


Fig. 5. Electron micrograph of BDA-labeled endings in the subpeduncular corner. The dark DAB reaction product is clearly evident. This particular ending appeared as a string of en passant swellings when viewed in the light microscope but was considerably more complicated with respect to its shape and contacts when viewed with the electron microscope. Scale bar = 1 μ m.

trols and lend credence to our observations of the additional projection to the cochlear nucleus. The application of a more sensitive dye coupled with a greater amount of dye injected seems to account for the greater details in this projection. There was a hint of this projection with wheat germ agglutinin conjugated with horseradish peroxidase where labeled axons were located in a triangular nuclear area between the trigeminal tract, inferior cerebellar peduncle, and ventral cochlear nucleus as well as in the

ventral cochlear nucleus itself (Pfaller and Arvidsson, 1988). The region described by Pfaller and Arvidsson corresponds closely to what has been called the *subpeduncular corner* (Mugnaini et al., 1980b; our Fig. 7).

Cellular targets

The labeled endings formed synapses with presumptive dendrites of granule cells, dendrites of UBCs, and axon terminals containing pleomorphic synaptic vesicles (see

TABLE 1. Summary of Postsynaptic Targets by DRG Endings in the Cochlear Nucleus

| Ending—Rat number | GCD target types and number of PSD contacts on separate targets | | | EM sections examined |
|-------------------|---|-----------------|-------------------------|----------------------|
| | UBC dendrite | Axonal terminal | Presumptive GC dendrite | |
| 1—Rat 1 | 3 | 4 | 18 | 45 |
| 2—Rat 1 | | 5 | 7 | 62 |
| 3—Rat 1 | | | 1 | 11 |
| 4—Rat 1 | | | 1 | 20 |
| 5—Rat 1 | | | 1 | 15 |
| 6—Rat 1 | | | 1 | 2 |
| 7—Rat 1 | | | 3 | 2 |
| 8—Rat 1 | | 1 | 5 | 15 |
| 9—Rat 1 | 1 | 3 | 4 | 43 |
| 10—Rat 1 | | 1 | 5 | 27 |
| 11—Rat 1 | | | 1 | 6 |
| 12—Rat 1 | | | 3 | 33 |
| 13—Rat 1 | | | 2 | 14 |
| 14—Rat 1 | 1 | 3 | 4 | 22 |
| 15—Rat 1 | | | 3 | 20 |
| 16—Rat 2 | 1 | | 1 | 44 |
| 17—Rat 3 | | | 3 | 48 |
| 18—Rat 3 | | 1 | 3 | 48 |
| 19—Rat 3 | | | 4 | 27 |
| 20—Rat 3 | 1 | | 1 | 14 |
| 21—Rat 3 | | | 1 | 1 |
| 22—Rat 3 | | 1 | | 2 |
| 23—Rat 3 | 1 | | 6 | 2 |

Table 1). Two endings formed synapses with both UBC dendrites and axon terminals containing pleomorphic vesicles. The granule cell identification was inferred on the basis of a dendritic arrangement with postsynaptic structures that resembled a “dendritic claw” and the presence of dendritic hairs that protruded into the ending (Fig. 8B). The dendrites of UBCs were identifiable by the presence of polyribosomes. Unequivocal proof of the target came from a fortuitous section that included the labeled synapse, the postsynaptic dendrite with ribosomes, and the UBC cell body. Three-dimensional reconstructions of the dendrite and terminal were made by using computer software and revealed that multiple dendrites branched from the primary dendrite, resembling a palm frond (data not shown) and typical of the UBC (Mugnaini and Floris, 1994; Wright et al., 1996).

The observation of DRG synapses upon axon terminals is novel but reliable and unambiguous. One-third of the labeled endings in our study made synaptic contact with an unlabeled axon terminal that contained pleomorphic synaptic vesicles. These terminals could be seen to arise from unmyelinated axons. Moreover, serial-section analysis, sometimes of up to 62 consecutive sections, confirmed that we were not examining dendrites that contain synaptic vesicles (Ralston et al., 1984; Peters et al., 1991). Labeled DRG terminals exhibited synaptic vesicles in close proximity (within a vesicle diameter or 50 nm) to the “presynaptic” membrane. Along the opposing membrane, there was a thickening and no nearby synaptic vesicles. These features led us to conclude that the labeled DRG terminal was presynaptic and that the unlabeled terminal with pleomorphic vesicles and a membrane thickening was postsynaptic.

Granule cells (Manis, 1989; Hunter et al., 1993; Rubio and Wenthold, 1997; Rubio and Juiz, 1998; Chen et al., 1999) and UBCs (Nunzi et al., 2001) are glutamatergic and are thought to be excitatory. Synaptic endings with pleomorphic synaptic vesicles are associated with the inhibitory neurotransmitters glycine and γ -aminobutyric acid (GABA; Juiz et al., 1996; Rubio and Juiz, 2004).

Consequently, neither granule cells nor UBCs are likely to be the source of the terminals postsynaptic to the DRG endings. There are two implications for these data in the cochlear nucleus: 1) The DRG terminals target at least three different neuronal structures, and 2) there are axoaxonic synapses of excitatory terminals on inhibitory terminals, which could represent presynaptic inhibition and ultimately increased excitability in the nucleus.

Axoaxonic relationships

Axoaxonic synapses were originally described in the spinal cord (Gray, 1962), and their presence supported a mechanism for presynaptic inhibition called “primary afferent depolarization” (Eccles et al., 1961). It should be noted that axoaxonic terminals have been described in the dorsal and ventral horns of the spinal cord (Watson and Bazzaz, 2001; Watson et al., 2002) and in the principal sensory nucleus of the trigeminal nucleus (Bae et al., 2005), where the presynaptic terminal contains pleomorphic terminals and immunostains for GABA and glycine. Physiological recordings at nerve terminals during presynaptic inhibition have suggested that the amplitude of the invading excitatory action potential is reduced during presynaptic inhibition because of a conductance change induced in the postsynaptic nerve terminal by the transmitter (Takeuchi and Takeuchi, 1966; Katz and Miledi, 1967; Baxter and Bittner, 1981; Segev, 1990). The inhibitory transmitter GABA is thought to generate a depolarizing response by causing an outward flux of chloride ions that produces the primary afferent depolarization and reduced transmitter release. This sequence is termed *presynaptic inhibition* (Rudomin, 1999).

It should be noted that our observation of “excitatory” terminals synapsing on “inhibitory” terminals raises questions regarding the effect of this synaptic arrangement and its possible mechanisms. One idea is that presynaptic depolarization directly reduces Ca^{2+} influx and reduces transmitter release (Malenka and Siegelbaum, 2001). Another proposal is that depolarization increases the influx of Ca^{2+} and causes an increase in neurotransmitter release (Radcliffe et al., 1999). These alternate views depend heavily on the presynaptic transmitter and the types and distributions of transmitter receptors.

GABA is the major inhibitory neurotransmitter in the central nervous system. The response to GABA is a rapid, chloride-mediated membrane hyperpolarization when GABA_A receptors are involved and a slower hyperpolarization mediated via GABA_B receptors caused by an efflux of K^{+} from the cell. Because GABA_B receptors can be found on both the pre- and the postsynaptic membrane, they have been implicated in many neuronal processes (Misgeld et al., 1995; Couve et al., 2000). If the DRG afferents terminate on GABAergic terminals, then the presence of presynaptic GABA_B could be viewed as a means to regulate the release of GABA from the terminals (Misgeld et al., 1995). This kind of “autoreceptor” could provide negative feedback control of GABA release. Regardless, it remains to be determined what neurotransmitters and receptors are involved.

The asymmetric nature of the membrane specializations and the round shape of the vesicles in the DRG endings imply an excitatory synapse. The excitation is expected to have a depolarizing effect on the postsynaptic inhibitory terminal, although, given the novelty of our observations, there are no data to confirm or refute any

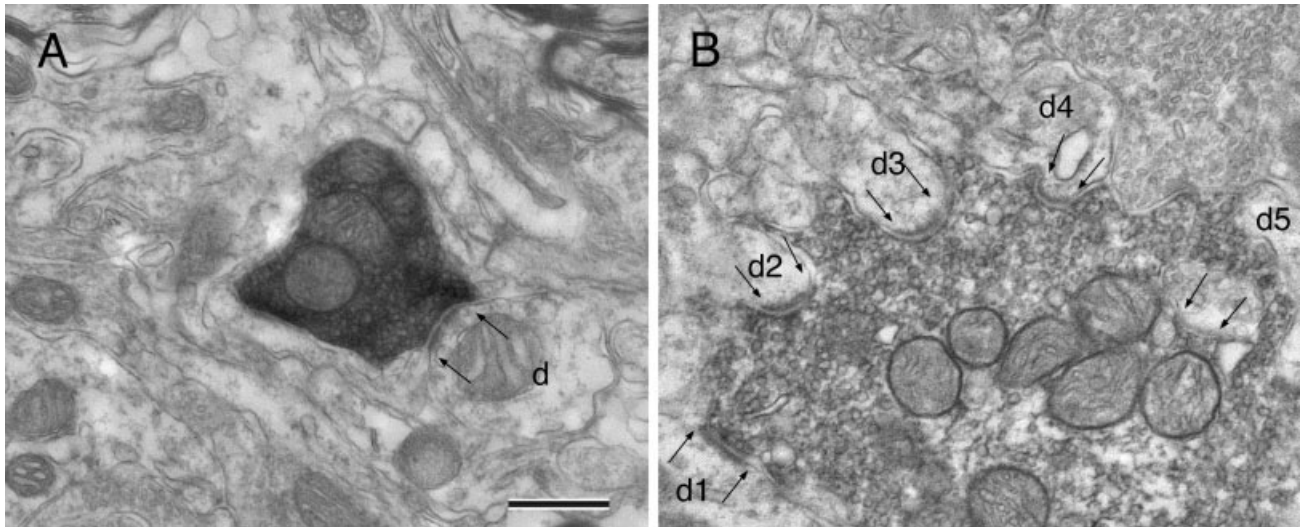


Fig. 6. Electron micrographs of labeled endings that synapse on dendrites. **A:** This synapse (arrows) is asymmetric and upon a thin dendrite (d) of unknown origin but having features of a granule cell. **B:** A larger ending formed a synapse on each of an array of dendrites

(d1–d5). This relationship resembled that of a mossy fiber with dendrites of a granule cell “claw.” Asymmetric synapses are indicated by arrows. Scale bar = 0.5 μm in A (applies to A,B).

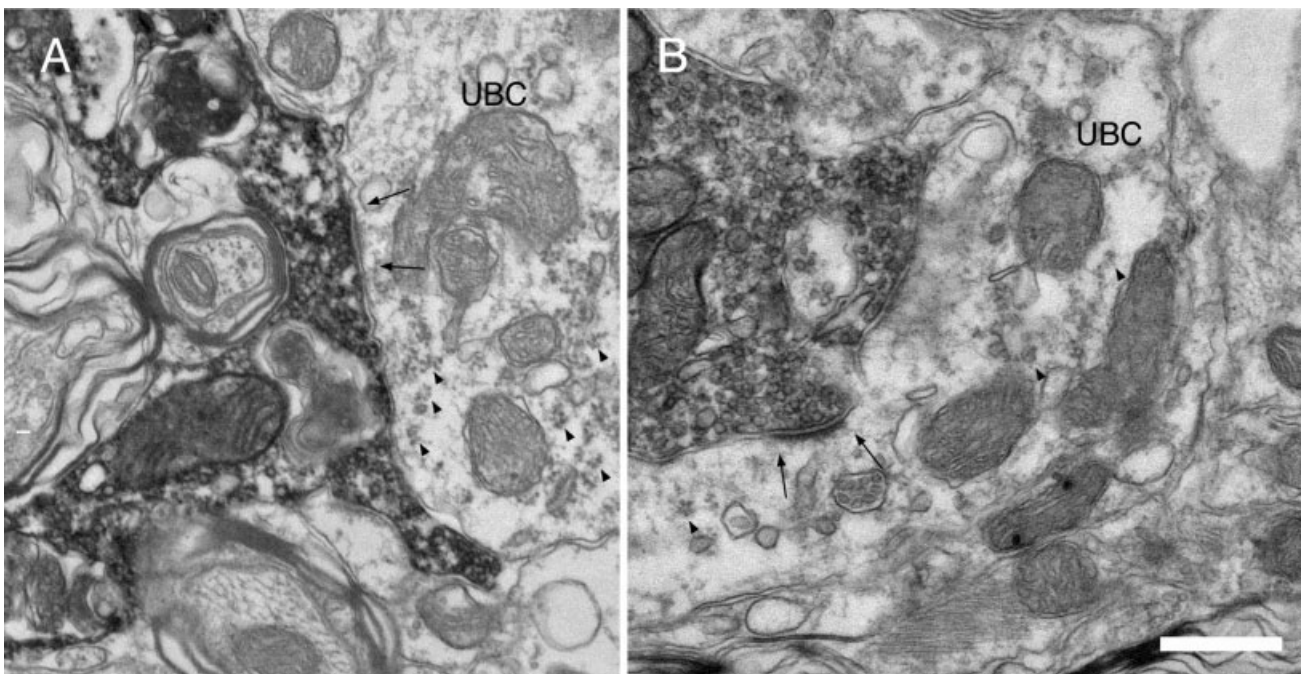


Fig. 7. **A,B:** Electron micrographs of labeled endings that synapse on dendrites that contain ribosomes (arrowheads). Dendrites with ribosomes (polyribosomes) had been attributed to unipolar brush cells (UBC) in previous reports (Jaarsma et al., 1996). The synapses (arrows) are of the asymmetric variety. Scale bar = 0.5 μm in B (applies to A,B).

speculations. This depolarizing effect on the postsynaptic axon terminal could presumably serve to reduce the amplitude of the action potentials at the release site and have an inhibitory effect as in the more conventional axoaxonic synapses. Because the postsynaptic terminals contain pleomorphic synaptic vesicles, we infer that there would be inhibitory effects on an inhibitory terminal.

Functional implications

UBCs are a unique class of excitatory, glutamatergic interneurons (Mugnaini and Floris, 1994; Floris et al., 1994; Jaarsma et al., 1995; Weedman et al., 1996; Mugnaini et al., 1997; Diño et al., 2000). They are distributed in the GCD of the cochlear nucleus and in the cerebellar

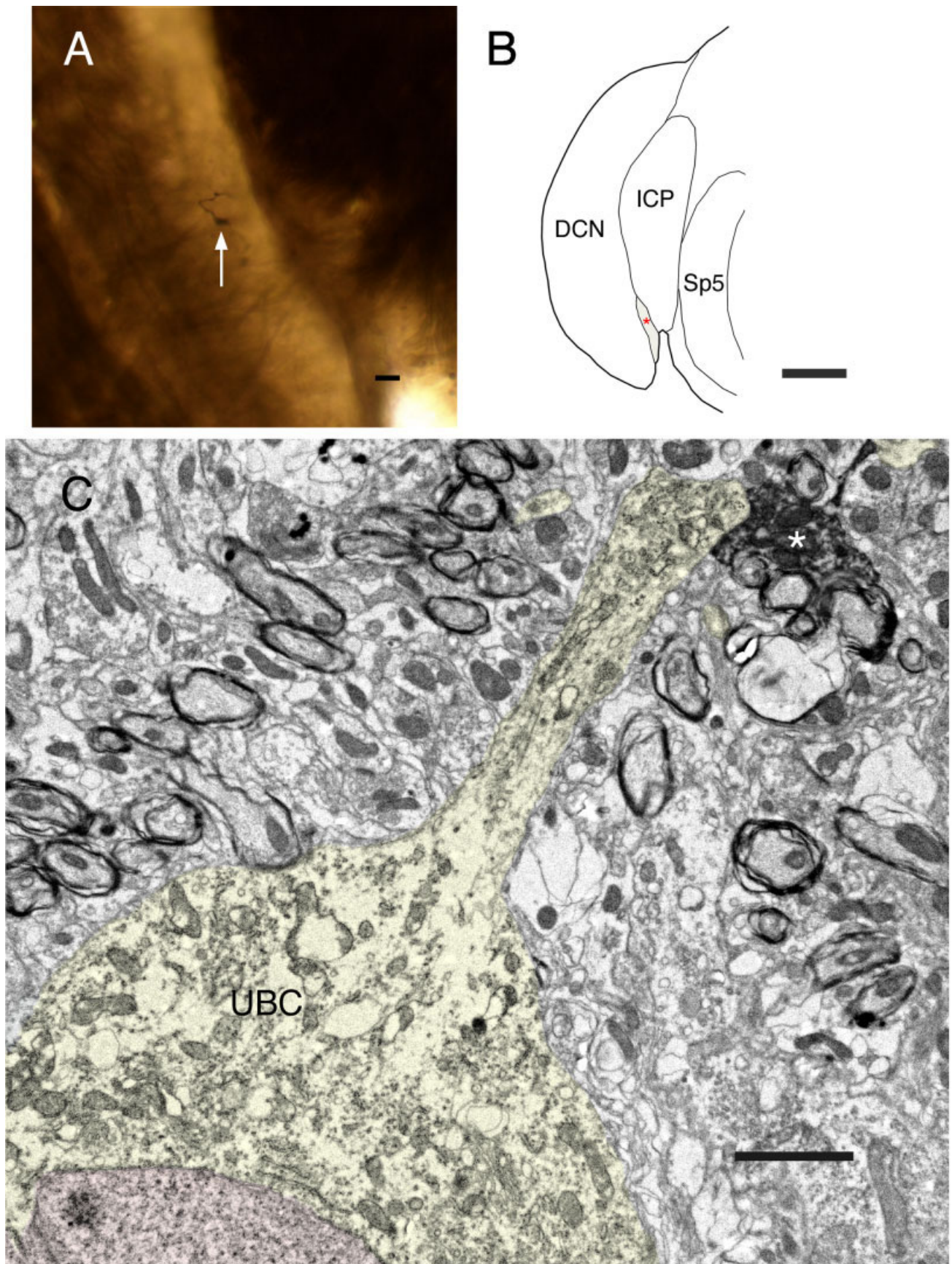


Fig. 8. C2 DRG projection terminates on a unipolar brush cell (UBC). **A:** Light photomicrograph of BDA-labeled terminal in the subpeduncular corner (arrow). **B:** Drawing of cochlear nucleus illustrating location of labeled terminal (asterisk). Abbreviations are provided in the legend for Figure 4. **C:** Electron micrograph of labeled ending (asterisk) forming a synapse on the dendrite of a unipolar brush cell (UBC). This dendrite (yellow) is directly connected to the

cell body, where the nucleus (pale red) exhibits a deep invagination of its envelope. Ribosomes are evident in the cell body and the dendrite. Dendrites (yellow) that branch off the main stalk as determined from serial section analysis are also shown. The morphology of the dendrites is a key feature of the UBC. Scale bars = 10 μm in A; 0.5 mm in B; 2 μm in C.

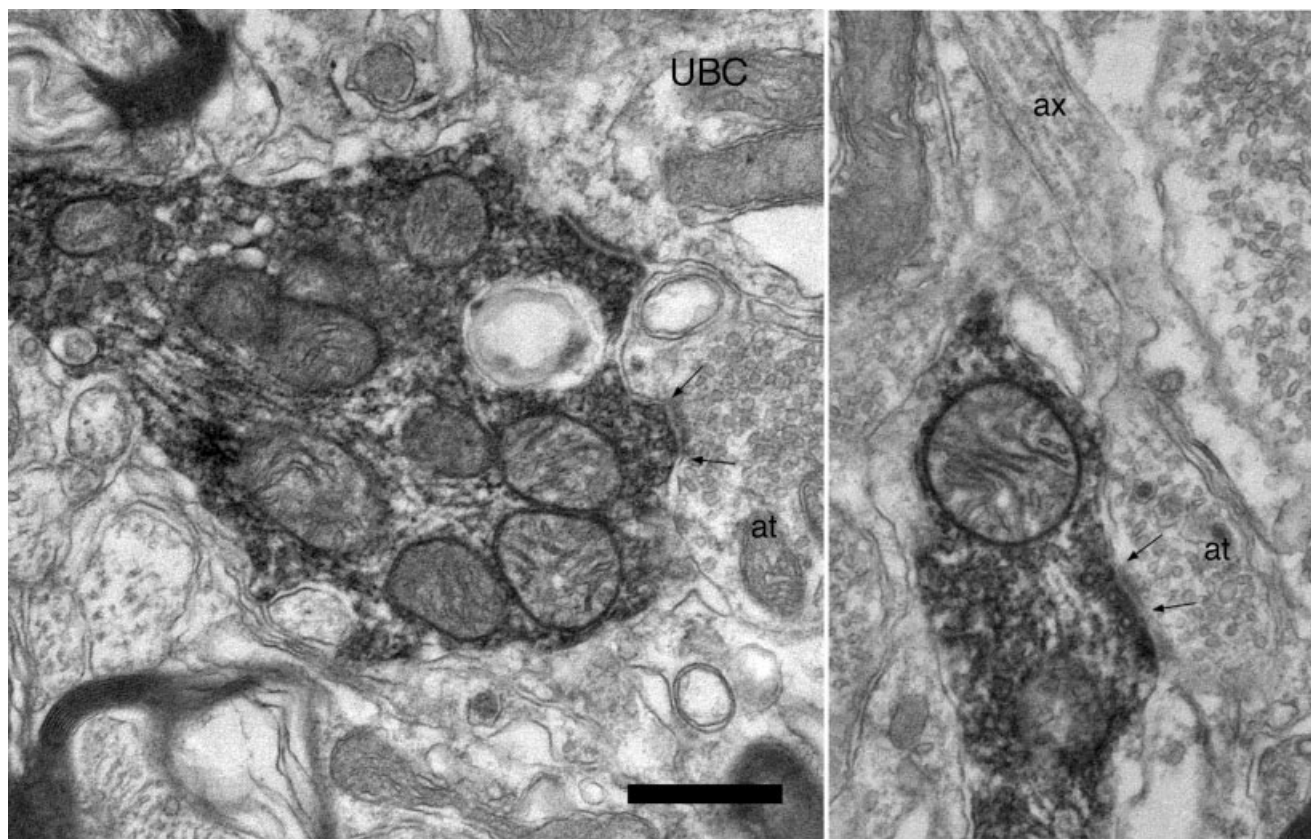


Fig. 9. Electron micrographs of endings forming asymmetric synapses (arrows) on structures containing pleomorphic synaptic vesicles. These target structures are called *axon terminals* (at) because of the vesicular content and continuity with axons (ax). Many of these postsynaptic terminals also contained vesicles with dense cores. Scale bar = 0.5 μ m (applies to all).

cortex. They receive a giant synapse from individual mossy fibers that is enclosed within a capsule of UBC dendrites (Weedman et al., 1996; Diño and Mugnaini, 2000). In turn, the UBC axons generate local circuit mossy fibers that form synaptic rosettes with the dendrites of other UBCs or granule cells (Diño et al., 2000; Nunzi et al., 2001; Kalinichenko et al., 2005). UBCs are thought of as “signal amplifiers” in that a single input spike produces multiple output spikes along an axon with multiple mossy fiber endings (Diño et al., 2000). The multiplication of spikes and the divergence of mossy fiber endings allow UBCs to initiate a powerful excitatory “feed-forward” circuit that utilizes direct or indirect projections to principal cells of the DCN. The combination of excitatory input to the UBC dendrites and presynaptic inhibition of inhibitory terminals emphasizes the excitatory nature of this circuit. UBCs also appear to deliver highly integrated information to their targets, insofar as they receive diverse projections from multiple sources (Diño et al., 2000; Ohlrogge et al., 2001; Haenggeli et al., 2005).

Positional information from the head and neck provide important cues for sound localization (Oertel and Young, 2004). Stimulation of C2 DRG, cuneate nucleus, trigeminal nucleus, and parallel fibers in the DCN produced identical effects on the principal cells in the cat DCN (Young et al., 1995; Davis et al., 1996; Kanold and Young,

2001). Our findings, along with other data from anatomical tracings (Wright et al., 1996; Haenggeli et al., 2005), imply that there are multiple parallel pathways modulating somatosensory contribution to the auditory system: a direct pathway from C2 DRG to the CN and a polysynaptic pathway that includes the dorsal column nuclei. Our electrical activation of the DRG produced complex evoked potential in the cochlear nucleus, which was consistent with previous findings (Kanold and Young, 2001) and suggested the presence of a similar anatomical pathway in the rat auditory system. Although the rat's pinnae are less mobile than those of cats, proprioceptive information about head and neck position are nonetheless important to this species.

The GCD is one of several auditory structures that receives inputs from nonauditory sources. The external cortex of the inferior colliculus (RoBards, 1979; Tokunaga et al., 1984; Paloff and Usunoff, 1992; Li and Mizuno, 1997a,b) and the medial division of the medial geniculate nucleus (Weptic, 1966; Lund and Webster, 1967; Schroeder and Jane, 1971) are also involved in the integration of multimodal afferents with auditory signals. The convergence of nonauditory inputs to auditory structures along the neuraxis accentuates the integrative nature of hearing.

Our anatomical results demonstrated a direct projection from C2 DRG to the GCD of cochlear nucleus. The direct projection provides a faster means for the auditory system to code sensory information about the neck, head, and pinna. The complex nature of the evoked response from DRG stimulation (Kanold and Young, 2001) could be attributed to the direct and indirect projection from C2 DRG as well as the interactions of multiple recipients of this input within the cochlear nucleus. However, it is not known yet to what extent or how these parallel projections converge to the principal cells of DCN. Presumably, these projections provide information to the principal cells regarding the relative position of the head and pinna with respect to the sound source. The data are consistent with the idea that somatosensory information from C2 DRG may contribute to spectral processing of auditory responsive neurons in the cochlear nucleus for sound location (for review see Oertel and Young, 2004).

A puzzling and progressive diminution of distinct cell layers in the DCN has been reported for primates, beginning with prosimians, continuing with monkeys, and concluding with humans (Füese, 1913; Moskowitz, 1967; Moore and Osen, 1979; Moore, 1980; Heiman-Patterson and Strominger, 1985). The change in DCN organization is attributed, at least in part, to a reorganization or loss of granule cells. There appears to be a similar diminution of DCN stratification in aquatic (porpoises: Osen and Jansen, 1965) and certain aerial (bats: Feng and Vater, 1985) mammals. A comparative study of the DCN of mammals inhabiting highly specialized environmental niches could yield insight into the functional significance of granule cells and DCN lamination. Ultimately, we would like to know whether granule cells in these species disappear or simply have a different distribution or organization.

Considerations of somatic tinnitus

Somatic tinnitus has been attributed to pathways involving the cuneate and spinal trigeminal nuclei because movement of the jaw and/or neck; touching of the face, scalp, or nape; and isotonic contractions of facial muscles can alleviate the perception of tinnitus (Levine, 1999, 2004; Sanchez et al., 2002; Levine et al., 2003; Abel and Levine, 2004). These clinical examples emphasize functional interactions between the somatosensory and the auditory systems. Because the human lacks a prominent GCD, however, the nature somatic modulation of tinnitus remains to be determined.

ACKNOWLEDGMENTS

The authors thank Nell Cant, Tom Parks, Alan Peters, Noah Meltzer, and Marc Eisen for their helpful discussions. Karen Montey and San-san Yu provided outstanding technical help.

LITERATURE CITED

- Abel MD, Levine RA. 2004. Muscle contractions and auditory perception in tinnitus patients and nonclinical subjects. *Cranio* 22:181–191.
- Abrahams VC, Richmond FJ, Keane J. 1984. Projections from C2 and C3 nerves supplying muscles and skin of the cat neck: a study using transganglionic transport of horseradish peroxidase. *J Comp Neurol* 230:142–154.
- Bae YC, Park KS, Bae JY, Paik SK, Ahn DK, Moritani M, Yoshida A, Shigenaga Y. 2005. GABA and glycine in synaptic microcircuits associated with physiologically characterized primary afferents of cat trigeminal principal nucleus. *Exp Brain Res* 162:449–457.
- Baxter DA, Bittner GD. 1981. Intracellular recordings from crustacean motor axons during presynaptic inhibition. *Brain Res* 233:422–428.
- Chen K, Waller HJ, Godfrey TG, Godfrey DA. 1999. Glutamergic transmission of neuronal responses to carbachol in rat dorsal cochlear nucleus slices. *Neuroscience* 90:1043–1049.
- Couve A, Moss SJ, Pangalos MN. 2000. GABA_B receptors: a new paradigm in G protein signaling [review]. *Mol Cell Neurosci* 16:296–312.
- Davis KA, Miller RL, Young ED. 1996. Effects of somatosensory and parallel-fiber stimulation on neurons in dorsal cochlear nucleus. *J Neurophysiol* 76:3012–3024.
- Diño MR, Mugnaini E. 2000. Postsynaptic actin filaments at the giant mossy fiber-unipolar brush cell synapse. *Synapse* 38:499–510.
- Diño MR, Schuergler RJ, Liu Y, Slater NT, Mugnaini E. 2000. Unipolar brush cell: a potential feedforward excitatory interneuron of the cerebellum. *Neuroscience* 98:625–636.
- Eccles JC, Eccles RM, Magni F. 1961. Central inhibitory action attributable to presynaptic depolarization produced by muscle afferent volleys. *J Physiol* 159:147–166.
- Feng AS, Vater M. 1985. Functional organization of the cochlear nucleus of rufous horseshoe bats (*Rhinolophus rouxi*): frequencies and internal connections are arranged in slabs. *J Comp Neurol* 235:529–553.
- Floris A, Diño MR, Jacobowitz DM, Mugnaini E. 1994. The unipolar brush cells of the rat cerebellar cortex and cochlear nucleus are calretinin-positive: a study by light and electron microscopic immunocytochemistry. *Anat Embryol* 189:495–520.
- Füese G. 1913. Das Ganglion ventrale und das Tuberculum acusticum dei einigen Säuglingen und beim Menschen. *Arb Hirnant Inst Zürich* 7:1–210.
- Gray EG. 1962. A morphological basis for presynaptic inhibition? *Nature* 193:82–83.
- Haenggeli CA, Pongstaporn T, Doucet JR, Ryugo DK. 2005. Projections from the spinal trigeminal nucleus to the cochlear nucleus in the rat. *J Comp Neurol* 484:191–205.
- Heiman-Patterson TD, Strominger NL. 1985. Morphological changes in the cochlear nuclear complex in primate phylogeny and development. *J Morphol* 186:289–306.
- Hunter C, Petralia RS, Vu T, Wenthold RJ. 1993. Expression of AMPA-selective glutamate receptor subunits in morphologically defined neurons of the mammalian cochlear nucleus. *J Neurosci* 13:1932–1946.
- Itoh K, Kamiya H, Mitani A, Yasui Y, Takada M, Mizuno N. 1987. Direct projections from the dorsal column nuclei and the spinal trigeminal nuclei to the cochlear nuclei in the cat. *Brain Res* 400:145–150.
- Jaarsma D, Wenthold RJ, Mugnaini E. 1995. Glutamate receptor subunits at mossy fiber-unipolar brush cell synapses: light and electron microscopic immunocytochemical study in cerebellar cortex of rat and cat. *J Comp Neurol* 357:145–160.
- Jaarsma D, Diño MR, Cozzari C, Mugnaini E. 1996. Cerebellar choline acetyltransferase positive mossy fibres and their granule and unipolar brush cell targets: a model for central cholinergic nicotinic neurotransmission. *J Neurocytol* 25:829–842.
- Jaarsma D, Diño MR, Ohishi H, Shigemoto R, Mugnaini E. 1998. Metabotropic glutamate receptors are associated with non-synaptic appendages of unipolar brush cells in rat cerebellar cortex and cochlear nuclear complex. *J Neurocytol* 27:303–327.
- Juiz JM, Helfert RH, Bonneau JM, Wenthold RJ, Altschuler RA. 1996. Three classes of inhibitory amino acid terminals in the cochlear nucleus of the guinea pig. *J Comp Neurol* 373:11–26.
- Kalinichenko SG, Okhotin VE. 2005. Unipolar brush cells—a new type of excitatory interneuron in the cerebellar cortex and cochlear nuclei of the brainstem. *Neurosci Behav Physiol* 35:21–36.
- Kanold PO, Young ED. 2001. Proprioceptive information from the pinna provides somatosensory input to cat dorsal cochlear nucleus. *J Neurosci* 21:7848–7858.
- Katz B, Miledi R. 1967. A study of synaptic transmission in the absence of nerve impulses. *J Physiol* 192:403–436.
- Levine RA. 1999. Somatic (craniocervical) tinnitus and the dorsal cochlear nucleus hypothesis. *Am J Otolaryngol* 20:351–362.
- Levine RA. 2004. Somatic tinnitus. In: Snow J, editor. *Tinnitus: theory and management*. Hamilton, Ontario, Canada: B.C. Decker. p 108–124.
- Levine RA, Abel M, Cheng H. 2003. CNS somatosensory-auditory interactions elicit or modulate tinnitus. *Exp Brain Res* 153:643–648.
- Li H, Mizuno N. 1997a. Single neurons in the spinal trigeminal and dorsal

- column nuclei project to both the cochlear nucleus and the inferior colliculus by way of axon collaterals: a fluorescent retrograde double-labeling study in the rat. *Neurosci Res* 29:135–142.
- Li H, Mizuno N. 1997b. Collateral projections from single neurons in the dorsal column nuclei to both the cochlear nucleus and the ventrobasal thalamus: a retrograde double-labeling study in the rat. *Neurosci Lett* 222:87–90.
- Lund RD, Webster KE. 1967. Thalamic afferents from the spinal cord and trigeminal nuclei. An experimental anatomical study in the rat. *J Comp Neurol* 130:313–328.
- Malenka RC, Siegelbaum SA. 2001. Synaptic plasticity: diverse targets and mechanisms for regulating synaptic efficacy. In: Cowan WM, Sudhof TC, Stevens CF, editors. *Synapses*. Baltimore: Johns Hopkins University Press. p 393–453.
- Manis PB. 1989. Responses to parallel fiber stimulation in the guinea pig dorsal cochlear nucleus in vitro. *J Neurophysiol* 61:149–161.
- Misgeld U, Bijak M, Jarolimek W. 1995. A physiological role for GABA_B receptors and the effects of baclofen in the mammalian central nervous system. *Prog Neurobiol* 46:423–462.
- Moore JK. 1980. The primate cochlear nuclei: loss of lamination as a phylogenetic process. *J Comp Neurol* 193:609–629.
- Moore JK, Osen KK. 1979. The cochlear nuclei in man. *Am J Anat* 154:393–418.
- Moskowitz N. 1967. Comparative aspects of some features of the central auditory system of primates. *Am N Y Acad Sci* 167:357–369.
- Mugnaini E, Floris A. 1994. The unipolar brush cell: a neglected neuron of the cerebellar cortex. *J Comp Neurol* 16:174–180.
- Mugnaini E, Osen KK, Dahl AL, Friedrich VL Jr, Korte G. 1980a. Fine structure of granule cells and related interneurons (termed Golgi cells) in the cochlear nuclear complex of cat, rat, and mouse. *J Neurocytol* 9:537–570.
- Mugnaini E, Warr WB, Osen KK. 1980b. Distribution and light microscopic features of granule cells in the cochlear nuclei of cat, rat, and mouse. *J Comp Neurol* 191:581–606.
- Mugnaini E, Diño MR, Jaarsma D. 1997. The unipolar brush cells of the mammalian cerebellum and cochlear nucleus: cytology and microcircuits. *Prog Brain Res* 114:131–150.
- Neuhuber WL, Zenker W. 1989. Central distribution of cervical primary afferents in the rat, with emphasis on proprioceptive projections to vestibular, perihypoglossal, and upper thoracic spinal nuclei. *J Comp Neurol* 280:231–253.
- Newlands SD, Perachio AA. 2003. Central projections of the vestibular nerve: a review and single fiber study in the Mongolian gerbil. *Exp Brain Res* 60:475–495.
- Novikov LN. 2001. Labeling of central projections of primary afferents in adult rats: a comparison between biotinylated dextran amine, neurobiotin and *Phaseolus vulgaris*-leucoagglutinin. *J Neurosci Methods* 112:145–154.
- Nunzi MG, Birnstiel S, Bhattacharyya BJ, Slater NT, Mugnaini E. 2001. Unipolar brush cells form a glutamatergic projection system within the mouse cerebellar cortex. *J Comp Neurol* 434:329–341.
- Oertel D, Young ED. 2004. What's a cerebellar circuit doing in the auditory system? *Trends Neurosci* 27:104–110.
- Ohlrogge M, Doucet JR, Ryugo DK. 2001. Projections of the pontine nuclei to the cochlear nucleus in rats. *J Comp Neurol* 436:290–303.
- Osen KK, Jansen J. 1965. The cochlear nuclei in the common porpoise, *Phocoena phocoena*. *J Comp Neurol* 135:223–258.
- Paloff AM, Usunoff KG. 1992. Projections to the inferior colliculus from the dorsal column nuclei. An experimental electron microscopic study in the cat. *J Hirnforsch* 33:597–610.
- Pannese E. 1981. The satellite cells of the sensory ganglia. *Adv Anat Embryol Cell Biol*, vol 65.
- Paxinos G, Watson C. 1998. *The rat brain in stereotaxic coordinates*, 4th ed. New York: Academic Press.
- Peters A, Palay SF, Webster HdeF. 1991. *The fine structure of the nervous system: neurons and their supporting cells*. New York: Oxford University Press.
- Pfaller K, Arvidsson J. 1988. Central distribution of trigeminal and upper cervical primary afferents in the rat studied by anterograde transport of horseradish peroxidase conjugated to wheat germ agglutinin. *J Comp Neurol* 268:91–108.
- Prihoda M, Hiller M-S, Mayr R. 1991. Central projections of cervical primary afferent fibers in the guinea pig: an HRP and WGA/HRP tracer study. *J Comp Neurol* 308:418–431.
- Radcliffe KA, Fisher JL, Gray R, Dani JA. 1999. Nicotinic modulation of glutamate and GABA synaptic transmission in hippocampal neurons. *Ann N Y Acad Sci* 868:591–610.
- Ralston HJ, Light AR, Ralston DD, Perl ER. 1984. Morphology and synaptic relationships of physiologically identified low-threshold dorsal root axons stained with intra-axonal horseradish peroxidase in the cat and monkey. *J Neurophysiol* 51:777–792.
- Rambourg A, Clermont Y, Beaudet A. 1983. Ultrastructural features of six types of neurons in rat dorsal root ganglia. *J Neurocytol* 12:47–66.
- RoBards MJ. 1979. Somatic neurons in the brainstem and neocortex projecting to the external nucleus of the inferior colliculus: anatomical study in the opossum. *J Comp Neurol* 184:547–566.
- Rubio ME, Juiz JM. 1998. Chemical anatomy of excitatory endings in the dorsal cochlear nucleus of the rat: differential synaptic distribution of aspartate aminotransferase, glutamate, and vesicular zinc. *J Comp Neurol* 399:341–358.
- Rubio ME, Juiz JM. 2004. Differential distribution of synaptic endings containing glutamate, glycine, and GABA in the rat dorsal cochlear nucleus. *J Comp Neurol* 477:253–272.
- Rubio ME, Wenthold JR. 1997. Glutamate receptors are selectively targeted to postsynaptic sites in neurons. *Neuron* 18:939–950.
- Rudomin P. 1999. Presynaptic selection of afferent inflow in the spinal cord. *J Physiol* 93:329–347.
- Rustioni A. 2005. Modulation of sensory input to the spinal cord by presynaptic ionotropic glutamate receptors. *Arch Ital Biol* 143:103–112.
- Sanchez TG, Guerra GC, Lorenzi MC, Brandao AL, Bento RF. 2002. The influence of voluntary muscle contractions upon the onset and modulation of tinnitus. *Audiol Neurootol* 7:370–375.
- Schroeder DM, Jane JA. 1971. Projections of the dorsal column nuclei and spinal cord to brain stem and thalamus in the tree shrew (*Tupaia glis*). *J Comp Neurol* 142:309–350.
- Segev I. 1990. Computer study of presynaptic inhibition controlling the spread of action potentials into axonal terminals. *J Neurophysiol* 63:987–998.
- Steward O, Worley PF. 2001. A cellular mechanism for targeting newly synthesized mRNAs to synaptic sites on dendrites. *Proc Natl Acad Sci U S A* 98:7062–7068.
- Takeuchi A, Takeuchi N. 1966. On the permeability of the presynaptic terminal of the crayfish neuromuscular junction during synaptic inhibition and the action of gamma-aminobutyric acid. *J Physiol* 183:433–449.
- Tandrup T. 1995. Are the neurons in the dorsal root ganglion pseudounipolar? A comparison of the number of neurons and number of myelinated and unmyelinated fibres in the dorsal root. *J Comp Neurol* 357:341–347.
- Tandrup T. 2004. Unbiased estimates of number and size of rat dorsal root ganglion cells in studies of structure and cell survival. *J Neurocytol* 33:173–192.
- Tokunaga A, Sugita S, Otani K. 1984. Auditory and non-auditory subcortical afferents to the inferior colliculus in the rat. *J Hirnforsch* 25:461–472.
- Watson AHD, Bazzar AA. 2001. GABA and glycine-like immunoreactivity at axoaxonic synapses on Ia muscle afferent terminals in the spinal cord of the rat. *J Comp Neurol* 433:335–348.
- Watson AHD, Hughes DI, Bazzar AA. 2002. Synaptic relationships between hair follicle afferents and neurones expressing GABA and glycine-like immunoreactivity in the spinal cord of the rat. *J Comp Neurol* 452:367–380.
- Weedman DL, Pongstaporn T, Ryugo DK. 1996. Ultrastructural study of the granule cell domain of the cochlear nucleus in rats: mossy fiber endings and their targets. *J Comp Neurol* 369:345–360.
- Weinberg RJ, Rustioni A. 1987. A cuneocochlear pathway in the rat. *Neurosci* 20:209–219.
- Wepsic JG. 1966. Multimodal sensory activation of cells in the magnocellular medial geniculate nucleus. *Exp Neurol* 15:299–318.
- Wolff A, Künzle H. 1997. Cortical and medullary somatosensory projections to the cochlear nuclear complex in the hedgehog tenrec. *Neurosci Lett* 221:125–128.
- Wright DD, Ryugo DK. 1996. Mossy fiber projections from the cuneate nucleus to the cochlear nucleus in the rat. *J Comp Neurol* 365:159–172.
- Wright DD, Blackstone CD, Haganir RL, Ryugo DK. 1996. Immunocytochemical localization of the mGluR1 α metabotropic glutamate receptor in the dorsal cochlear nucleus. *J Comp Neurol* 364:729–745.
- Ye Y, Kim DO. 2001. Connections between the dorsal raphe nucleus and a hindbrain region consisting of the cochlear nucleus and neighboring structures. *Acta Otolaryngol* 121:284–248.
- Young ED, Nelken I, Conley RA. 1995. Somatosensory effects on neurons in dorsal cochlear nucleus. *J Neurophysiol* 73:743–765.